Calculational Support for the "No Excuses" KLOTZ Club Test at Linchburg Mine[*]

Lynn W. Kennedy
Charles E. Needham
Kenneth D. Schneider

Maxwell Laboratories, Inc., 5-Cubed Division
2501 Yale Blvd. S.E. Suite 300
Albuquerque, NM 87106

ABSTRACT

High resolution calculations have been performed to simulate the detonation and subsequent blast propagation of 37.3 kg/m^3 (TNT equivalent) of Comp B in an under-ground complex of chambers and tunnels like that of the Linchburg Mine near Magdalena, New Mexico. Tests were performed in this complex by the U.S. Army Water-ways Experiment Station (WES) in support of a joint US/ROK program and also for the KLOTZ Club.

The calculations were performed with S-Cubed's second-order, general-purpose Eulerian hydrocode, SHARC. Because of the importance of replicating a complex facility with high fidelity so that accurate predictions of blast waveforms can be made, not only within the detonation chamber and in nearby access tunnels, but in other chambers and at the remote mine portal, the calculation was undertaken in several stages. The first stage was a two-dimensional representation, in Cartesian coordinates, of the explosive detonation and surrounding chamber. For propagation throughout the complex, a two-dimensional Cartesian "plan view" representation was used. Finally, a two-dimensional cylindrical simulation was used to propagate the blast signal to the mine portal. Careful representation of grid-scale roughness elements of the mine walls were incorporated into the calculation.

The calculations are described, and results, in the form of station plots of measurable hydrodynamic parameters, are shown. The test was performed on 26 May, 1994. Limited, prelimininary comparisons between calculated and experimental results are made.

_____

Report Documentation Page

Public reporting burden for the collection of information is estimated to average 1 hour per response, including the time for reviewing instructions, searching existing data sources, gathering and maintaining the data needed, and completing and reviewing the collection of information. Send comments regarding this burden estimate or any other aspect of this collection of information, including suggestions for reducing this burden, to Washington Headquarters Services, Directorate for Information Operations and Reports, 1215 Jefferson Davis Highway, Suite 1204, Arlington VA 22202-4302. Respondents should be aware that notwithstanding any other provision of law, no person shall be subject to a penalty for failing to comply with a collection of information if it does not display a currently valid OMB control number.

1. REPORT DATE **AUG 1994**	2. REPORT TYPE	3. DATES COVERED **00-00-1994 to 00-00-1994**

4. TITLE AND SUBTITLE **Calculational Support for the 'No Excuses' KLOTZ Club Test at Linchburg Mine**	5a. CONTRACT NUMBER
	5b. GRANT NUMBER
	5c. PROGRAM ELEMENT NUMBER
6. AUTHOR(S)	5d. PROJECT NUMBER
	5e. TASK NUMBER
	5f. WORK UNIT NUMBER

7. PERFORMING ORGANIZATION NAME(S) AND ADDRESS(ES) **Maxwell Laboratories, Inc,5-Cubed Division,2501 Yale Blvd. S.E. Suite 300,Albuquerque,NM,87106**	8. PERFORMING ORGANIZATION REPORT NUMBER

9. SPONSORING/MONITORING AGENCY NAME(S) AND ADDRESS(ES)	10. SPONSOR/MONITOR'S ACRONYM(S)
	11. SPONSOR/MONITOR'S REPORT NUMBER(S)

12. DISTRIBUTION/AVAILABILITY STATEMENT
Approved for public release; distribution unlimited

13. SUPPLEMENTARY NOTES
See also ADM000767. Proceedings of the Twenty-Sixth DoD Explosives Safety Seminar Held in Miami, FL on 16-18 August 1994.

14. ABSTRACT
see report

15. SUBJECT TERMS

16. SECURITY CLASSIFICATION OF:			17. LIMITATION OF ABSTRACT	18. NUMBER OF PAGES	19a. NAME OF RESPONSIBLE PERSON
a. REPORT **unclassified**	b. ABSTRACT **unclassified**	c. THIS PAGE **unclassified**	**Same as Report (SAR)**	**13**	

explosive storage.

TEST PROGRAM; BACKGROUND

The Linchburg Mine is an inactive lead and zinc mine located in the Magdalena Mountains, about 18 miles west of the town of Socorro in the State of New Mexico. Privately owned, it was leased to the U.S. Government in 1992 for the Underground Munitions Storage Test Project. The project is part of a joint United States/Republic of Korea cooperative research and development program for new underground ammunition storage technologies.

Two new "test adits" were mined to the north and south of the main drift between 200 and 250 meters from the portal. From these adits, several test chambers were excavated, as shown in Figure 1. A series of $^1/3$-scale explosive experiments is being performed to test the ability of the various chamber configurations to limit the escape of airblast and fragments in case of accidental detonation of stored explosives.

So far, five tests have been executed in the Linchburg complex, one in the main tunnel and the other four in Chamber #4 of the left adit, shown in Figure 2. Test 1 consisted of a single, 14.3-kg charge of cast Comp-B detonated between the two adits in the main tunnel. Its purpose was to provide experimental data for a calculational study of the effects of the rough tunnel walls on shock wave propagation. As can be seen in Figure 3, where the overlay is experimental over pressure vs. time data and the main plot shows the results of two hydrodynamic code calculations with different tunnel roughness simulations, the calculations were very successful at reproducing the measured wave-forms in Test 1.

Tests 2 through 5 consisted of various charges and loading densities detonated in Chamber #4. Loading densities ranged from 1 to 37.3 kg/m^3 TNT equivalent of cast Comp B, and all four tests provided good airblast data. Test 5, the largest of the four, consisted of 180 of the 14.3-kg cast Comp-B blocks, for a total charge weight of 2570 kg. This test has been designated as the vehicle for the "No Excuses" KLOTZ Club simulation calculations. This means that both calculators and experimenters were charged with providing their best possible results, with "no excuses" accepted on either side as to why those results were not the best that could be obtained. This does not mean, however, that the calculational techniques are perfect or that all the required physics is modeled. The calculations performed for this test simulation, done "blind" before the experimental results were made available to us, and comparison with the experimental data, are the subject of this paper.

CALCULATIONAL CONFIGURATION

The SHARC hydrodynamic code calculation for Test 5 was set up in five phases, in order to concentrate attention on different portions of the complex as required, and not to waste calculational resources on area/time regimes of limited interest. SHARC (SCubed Hydrodynamic Advanced Research Code) is a fully second-order, two- or three-dimensional,

multi-material hydrocode. All of the calculations done for this test were two-dimensional: the first three phases were run in a Cartesian coordinate system; the remaining two phases were transferred to cylindrical coordinates.

The first phase was a representation of only the detonation chamber (Chamber #4) and the detonating explosive. Figure 4 is a density contour plot just after initiation of the detonation. The entrance is at the top, and the explosive has been detonated at the end nearest the door. Note that an effort has been made to configure the chamber as it actually appeared when the test was performed. The earlier tests in the same chamber had loosened some of the material from the walls and ceiling, which was removed prior to Test #5. Thus the chamber was slightly bigger than originally planned. Information taken at the site just prior to the Test #5 detonation was used to modify the configuration. Zone dimensions for this phase were 2.5 x 2.5 cm.

At a time 0.5 ms after initiation of detonation, the results from the complete detonation in Chamber #4 were mapped into a larger grid including the entrance to Chamber #4 and part of the left adit tunnel. This phase, illustrated in Figure 5, used 5 x 5 cm zonal resolution. Both air and detonation products from the explosive were incorporated into this phase from the earlier detonation phase. Phase 2 covered the time period from 0.5 ms to 3 ms.

Phase 3 covered the entire left adit, as illustrated in Figure 6. This diagram included, to the extent possible, irregularities and as-built features in this portion of the underground complex. An example of our attempt to set up the calculation in a way that would closely model the actual configuration is given in Figures 7 and 8. Figure 7 is an as-built drawing of the entrance to Chamber #2. Figure 8, an overlay, is the computer model of this same area. The computer model is more irregular than the drawing, partly because we recognized that all of the actual irregularities could not be reproduced in the drawing, and partly because the boundaries in the calculation are constrained along cell edges. Note that the tunnel to Chamber #2 is narrower in the calculational representation. This is because the overhead in this tunnel was lower than that in the left adit. In a two-dimensional plan-view calculation, a unit height valid for all regions must be chosen; the tunnel must be made narrower to preserve the cross-sectional area under the unit height restriction.

Zone size for Phase 3 was 20 cm in the x-direction (horizontal) and 10 cm in the y-direction (vertical). Y-zone sizes were gradually increased with distance toward the top of the grid, so that Chambers #1, #2, and #3 were not as finely-zoned as the adit tunnel itself.

At a time of 43 ms, the calculation was converted from the Cartesian to a cylindrical coordinate system, in order to calculate propagation efficiently in the long, straight main tunnel from the adit to the portal. For this phase, a feed-in boundary for conditions from Phase 3 was established at the bottom of the mesh, with the portal at the top. Phase 3 had to be continued beyond this time, of course, in order to provide the feed-in conditions. Zone sizes for Phase 4 were 10 cm in the radial (x) direction and 20 cm in the axial (y) direction.

We used the same characterization for wall roughness, based on actual measurements, that we had developed for the calculation of Test 1. Figure 9 is a distorted view of the tunnel as set up for this phase of the calculation. The distortion ratio is 13/1 (axial distance/ radial distance) in order to allow the entire tunnel to be portrayed on a single plot. The extra chamber at y = 200 m is a simulation, in this coordinate system, of the right adit.

Finally, Phase 5 was begun, initiated from Phase 4 at 10 m from the portal at 430 ms. This phase was also set up in cylindrical coordinates, and was driven using the boundary feed-in technique with station records from Phase 4. It was designed to simulate airblast behavior outside the portal region. The calculational configuration is illustrated in Figure 10.

RESULTS

To demonstrate the results of the calculations, we have compared a selection of station records from the calculation with gage records obtained in the experiment. I want to emphasize again that this was a "blind" calculation; that is, we were not given access to the experimental records until the calculational results were delivered to the sponsors. We have not had time or funding to adjust the calculation or make any changes in input parameters since the data was received.

The first comparison is from Station 27, which is in the entrance passage to the detonation chamber (Figures 11 and 12). The arrival times are in agreement, and the over pressure peak values are not that different, about 23 MPa for the calculation and 19 MPa for the test. Quasi-static values near the end of the shock pulse (200 ms) are also similar, but in between there are some differences that we have not been able to explain, and these will also make a difference in the impulses. The calculation predicts significantly greater impulses than are observed in the test.

At Station 26, in the left adit just outside of the detonation chamber, again the arrival times and the late-time quasi-static pressures are in agreement, but the peak values differ by a factor of about three (Figures 13 and 14). In order to try to understand this, we looked at a contour plot of this region at 10 ms (Figure 15). Note that there is a standing wave formed by stagnation of flow on the wall opposite the chamber passageway. We found that, by moving to a calculational station further from the wall, outside of the standing-wave region, we could get better agreement between the two records (Figures 16 and 17). The experimental record shown in Figure 17 is the same as the one in Figure 14, but plotted to a different scale.

By the time we get to Station 17, which is also in the left adit, but at the entrance to Chamber #2, differences in arrival time are beginning to show up (Figures 18 and 19). The higher-pressure shock waves propagate more rapidly and hence arrive at a given station earlier. The differences m over pressure are about a factor of two for most of the record, although the peak experimental value is actually a little higher than anything in the calculation.

Finally, one comparison is shown from Station 7, in the main tunnel (Figures 20 and 21). Again, the calculation is early and high. We do not have a good explanation as to the reasons for this.

CONCLUSIONS

In undertaking this calculation, we made a significant effort to reproduce the "as built" characteristics of the tunnel complex. We also assured ourselves that a quality explosive was used for which we have a good equation-of-state. We are convinced that the hydrocode, including the explosive detonation routines, is working correctly. This has been tested over many years with numerous free-air experiments. We believe that we lived up to the "no excuses" requirement placed on us by our sponsors, in that we did the best job that we know how to do on this calculation.

However, as with all scientific endeavors, you do the best you can, using the best ideas and the best tools that are available, but sometimes you fall, or at least you are less successful than you had hoped to be. If this happens, there is nothing for it but to try to learn from your failures, generate better ideas and better tools, and try again.

To review our position: We have been successful in the past with small-scale experiments in smooth tunnels. We've also been successful with intermediate-scale experiments in rough tunnels, in which low explosive loading densities were used. An example of this is the Magdalena Test 1 comparisons. For the Test 5 investigation, we made a significant effort to measure and characterize wall roughness, and to measure and characterize as many features as possible of the "as built" facility. However, as for previous calculations with large loading densities in geologic materials, we have generally produced over pressure and dynamic pressure results that are too high, when compared to experimental data. These results are conservative from a safety analysis point of view.

So what should be the next step? We believe that, especially for large loading densities, there is a mechanism whereby energy can be removed from the blast wave that is not currently accounted for in the calculations. A number of possibilities have been suggested:

     1) Direct transfer of blast energy to ground displacement. Absorption of the energy may occur through crushing, dosing up of veins and fissures, or some other mechanism, or it may be by dissipation through the outward propagation of ground motion.

     2) Loss of heat energy by conduction into the rock walls of the chamber.

     3) Loss of energy to vaporization of water in the tunnel complex.

4) Trapping of energy in the wire mesh that is sometimes used to prevent sloughing off of the overburden.

5) Loss of energy to rock dust or other loose solid particulate in the tunnel complex, either by scouring/lofting or material vaporization.

Although we have looked at the first idea in some earlier tests with limited success, we have not combined this area of investigation with the rough-wall investigation. It may be that the appropriate combination of wall roughness and wall energy absorption would solve the problem, but both of these are infinitely variable, and it is hard to get a handle on the problem without a controlled set of data. It seems highly likely that both effects will depend on explosive loading density, but in different ways. Ground motion experts are generally of the opinion that only a few percent of the energy can be lost to ground motion in an uncoupled detonation.

The other ideas have been considered, but essentially nothing has been done to attempt to model them. The Linchberg mine Chamber #4 series may provide a set of data that can help to investigate these possibilities as functions of loading density. The series consists of three tests with cast Comp B, at loading densities of 1, 5, and 37.3 kg/m^3. It is the opinion of the authors that, by careful study of airblast records in and near the detonation chamber, and a few sample hydrocode calculations, models could be developed for energy trapping or absorption as a function of loading density, at least for the wiremesh covered Magdalena limestone of Chamber #4. Combining this model or models with the wall roughness characterization outlined and used here for propagation down long tunnels may allow the development of increased knowledge of effects associated with the detonation of explosives in underground facilities.
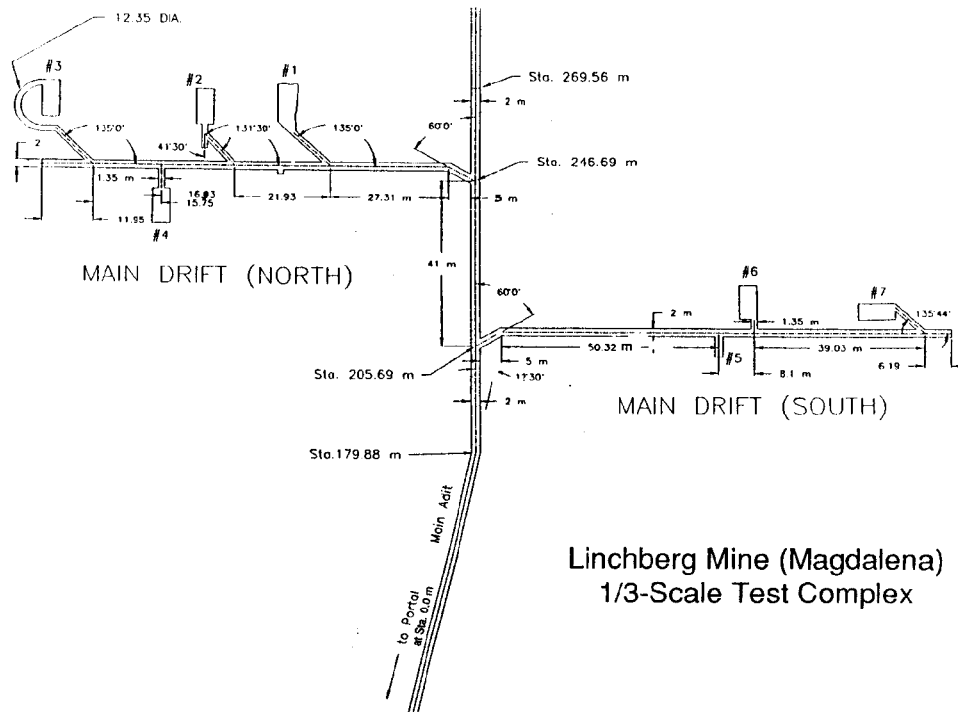
FIGURE 1. AND FIGURE 2.

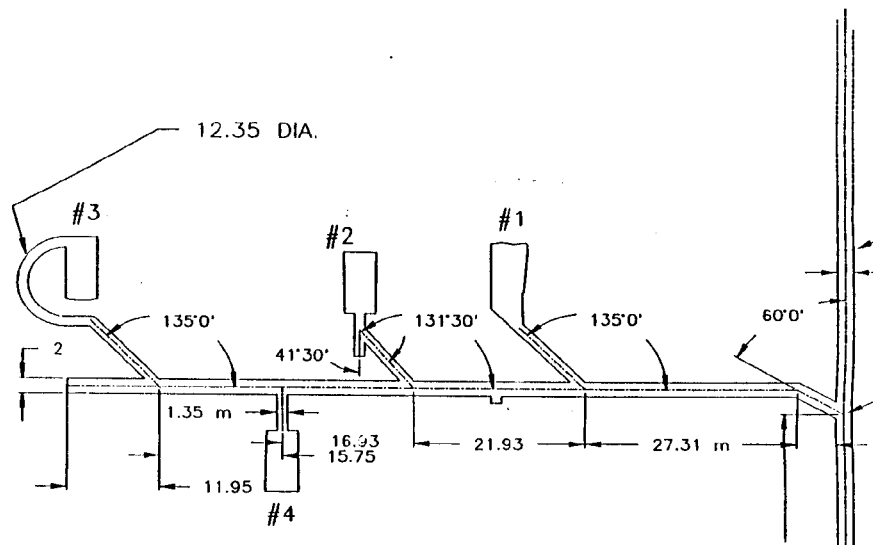Figure 1. Plan view of test adits and test chambers in Linchburg Mine

Figure 2. Detail view of left adit, with test chambers #1 through #4
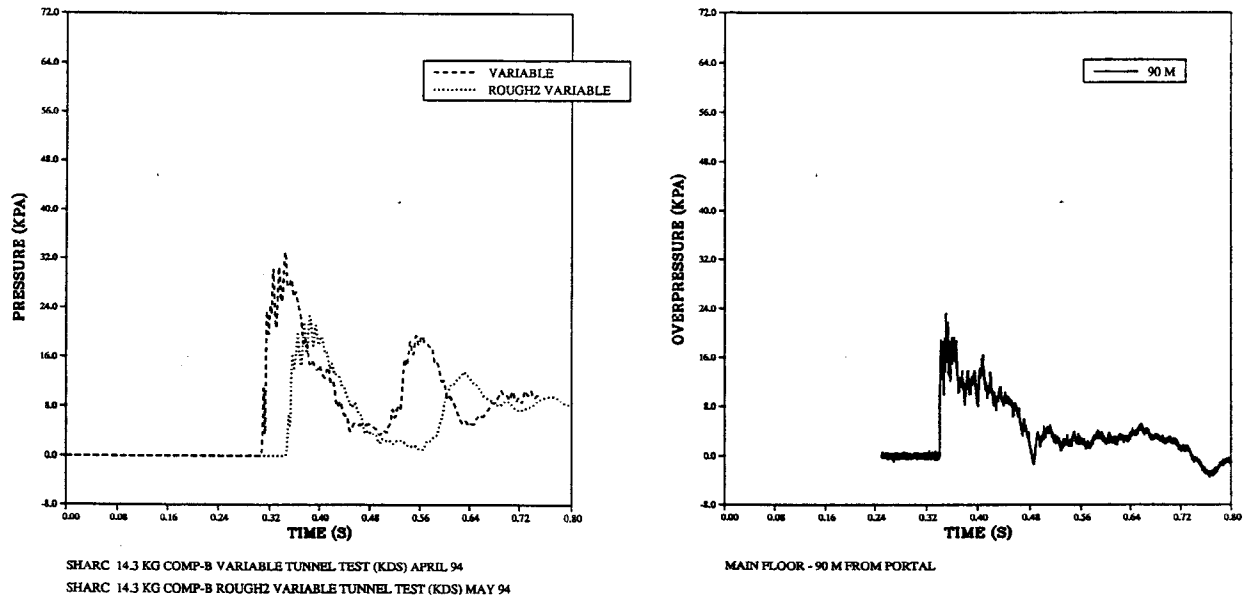
FIGURE 3., FIGURE 4. AND FIGURE 5.

SHARC 14.3 KG COMP-B VARIABLE TUNNEL TEST (KDS) APRIL 94
SHARC 14.3 KG COMP-B ROUGH2 VARIABLE TUNNEL TEST (KDS) MAY 94

MAIN FLOOR - 90 M FROM PORTAL

Figure 3. Station overpressure records from Test 1 at 90 m from the portal. The left-hand plot is calculational results from two different wall roughness configurations, the right-hand plot is the experimental data

LINCHBURG MINE   CHAMBER 4 DETONATION 2570 KG (KDS) MAY 94
TIME 100.000 USEC   CYCLE   225.   PROBLEM   25.0001

MAGDALENA CHAMBER 4 DETONATION 2570 KG (KDS) MAY 94
TIME   5.000 MSEC   CYCLE   753.   PROBLEM   25.0002
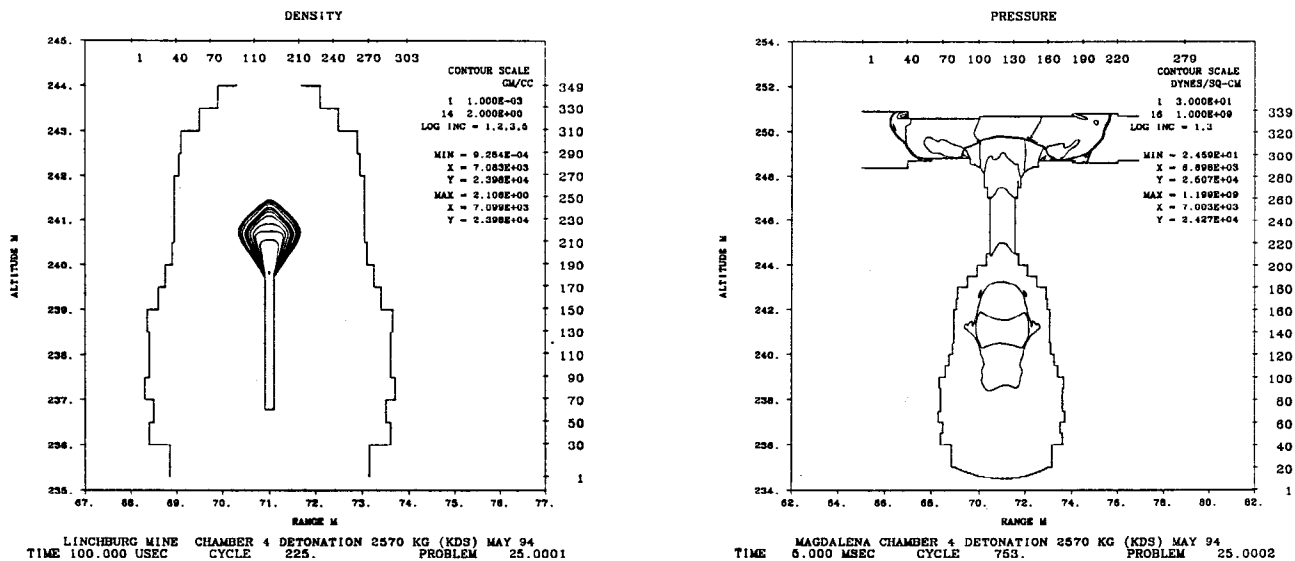
Figure 4. Density contour plot at 100 μs showing detonation of explosive in calculation Phase 1

Figure 5. Pressure contour plot at 5 ms showing expansion of shock into left adit, Phase 2

FIGURE 6., FIGURE 7. AND FIGURE 8.
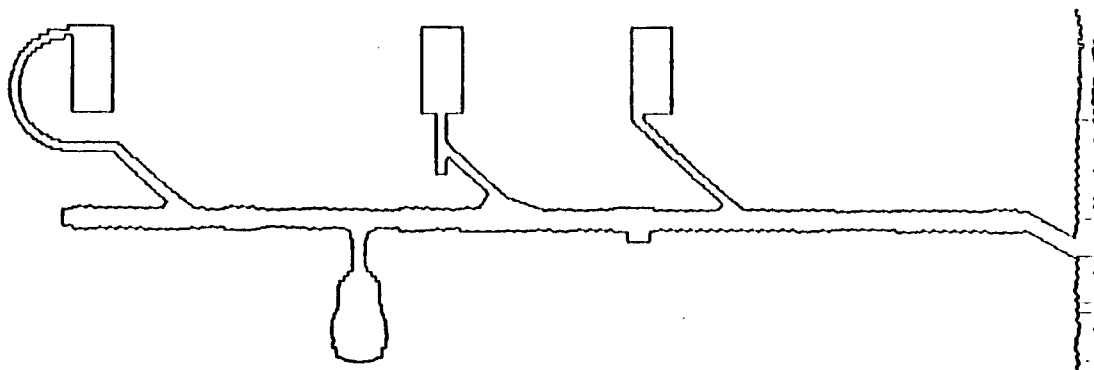
Figure 6. Left adit as-built, as modeled for calculation, Phase 3
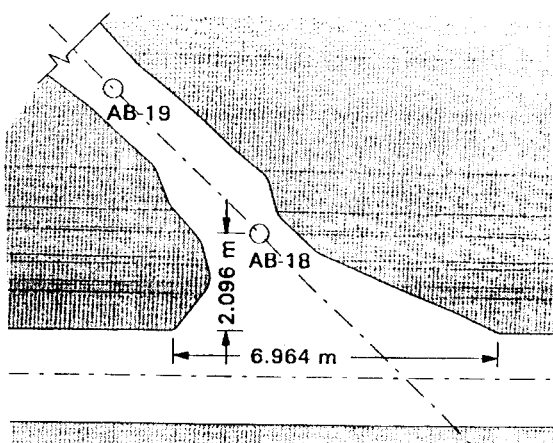
Figure 7. As-built drawing of the entrance to Chamber #2 access tunnel
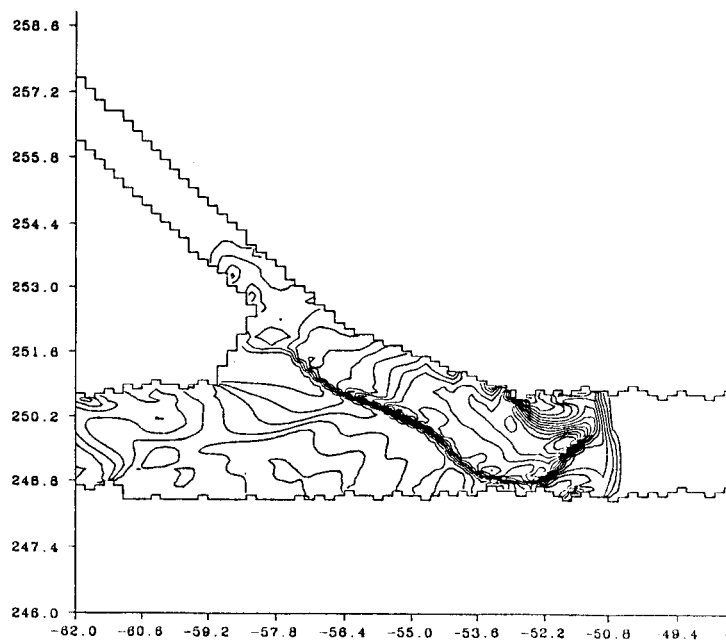
Figure 8. Calculational representation of the entrance to Chamber #2 access tunnel

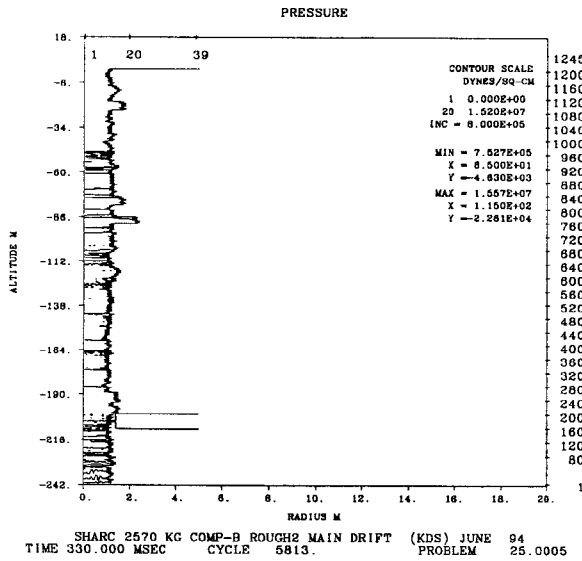# FIGURE 9., FIGURE 10. , FIGURE 11. AND FIGURE 12.

PRESSURE

CONTOUR SCALE
DYNES/SQ-CM

1   0.000E+00
20   1.520E+07
INC = 8.000E+05

MIN = 7.527E+05
X = 8.500E+01
Y = -4.630E+03

MAX = 1.557E+07
X = 1.150E+02
Y = -2.261E+04

SHARC 2570 KG COMP-B ROUGH2 MAIN DRIFT   (KDS) JUNE 94
TIME 330.000 MSEC   CYCLE   5813.   PROBLEM   25.0005

Figure 9. Distorted view of main tunnel as set up in cylindrical coordinates for the calculation, Phase 4. The portal is at the top

VELOCITY VECTORS

MAX VELOCITY = 4.26E+04 CM/S
VECTOR SCALE
1 IN = 5.000E+04 CM/S

MAGDALENA CHAMBER 4 2570 KG TURB EXTERIOR (KDS) JULY 94
TIME 490.034 MSEC   CYCLE   317.   PROBLEM   25.0006
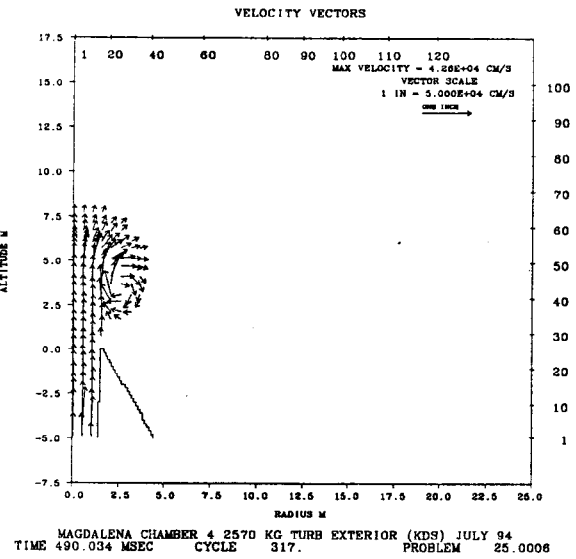
Figure 10. Velocity vector plot of the portal region, as set up in cylindrical coordinates for Phase 5 of the calculation

27-ABSO

27-ABSO

25.0004 STATION 2
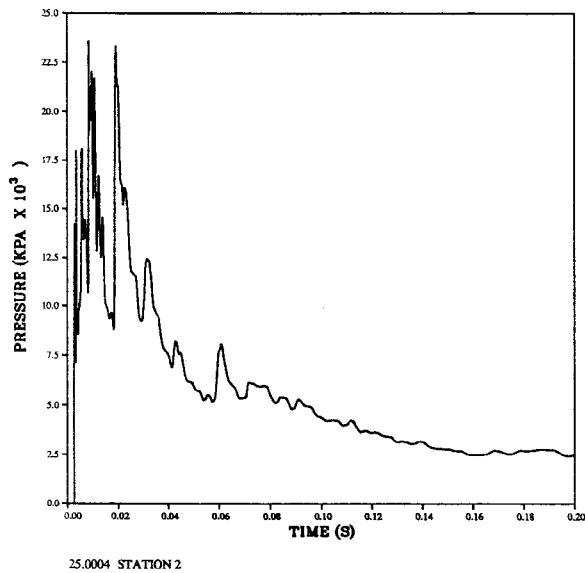
Figure 11. SHARC calculation overpressure record from Station 27, in the Chamber #4 entrance passage

TDR002.PRE
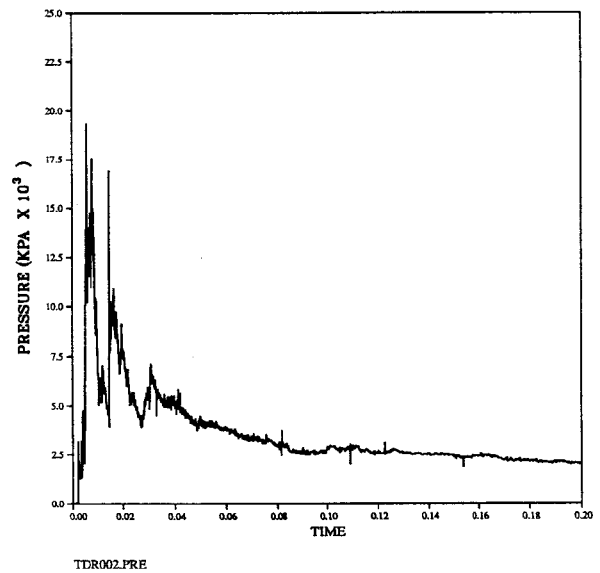
Figure 12. Experimental data overpressure record from Station 27, in the Chamber #4 entrance passage
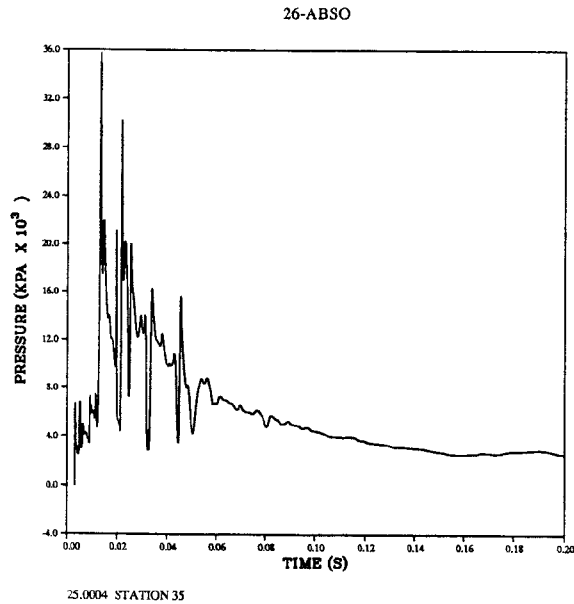
FIGURE 13., FIGURE 14. AND FIGURE 15.

26-ABSO

26-ABSO

25.0004 STATION 35

Figure 13. SHARC calculation
overpressure record from Station 26, in
the left adit near the entrance to
Chamber #4

TDR003.PRE
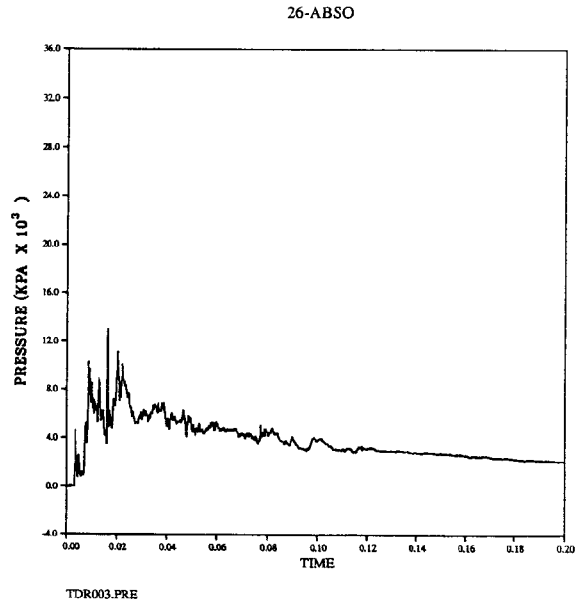
Figure 14. Experimental data
overpressure record from Station 26, in
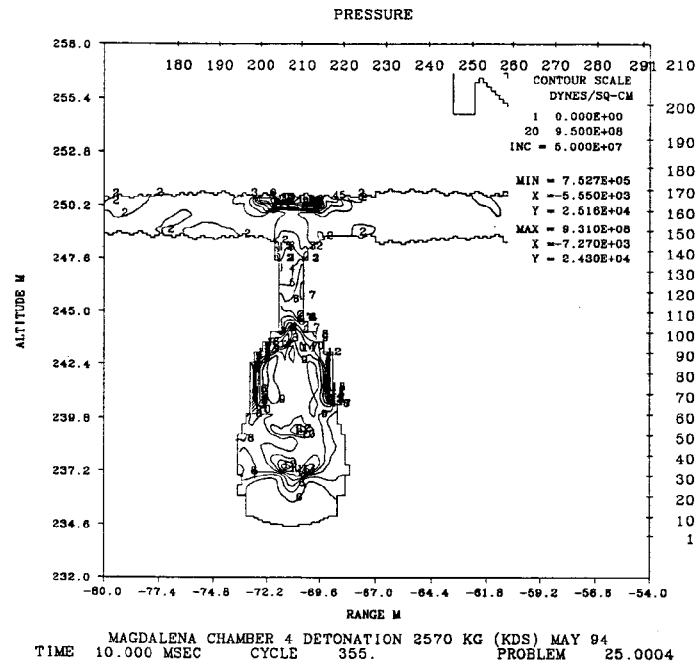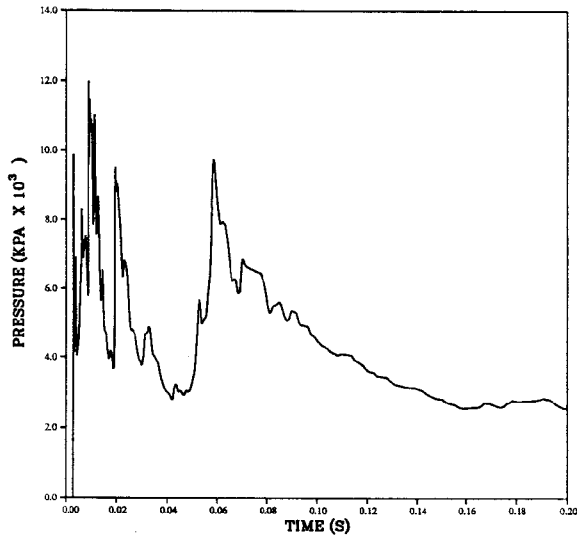the left adit near the entrance to
Chamber #4

PRESSURE

MAGDALENA CHAMBER 4 DETONATION 2570 KG (KDS) MAY 94
TIME   10.000 MSEC   CYCLE   355.   PROBLEM   25.0004

Figure 15. Pressure contour plot at 10 ms of Chamber #4 and a portion of the left adit,
showing standing wave against the wall opposite the entrance to Chamber #4

FIGURE 16., FIGURE 17. , FIGURE 18. AND FIGURE 19.

Figure 16. SHARC calculation overpressure record from a station in the left adit near the entrance to Chamber #4, but further from the wall than that shown in Figure 13
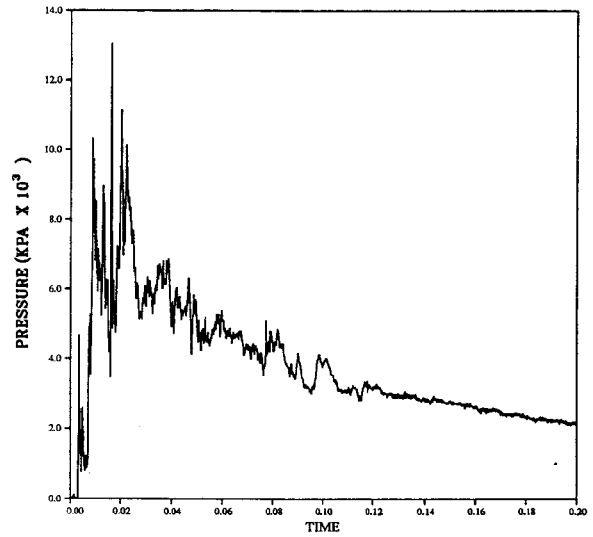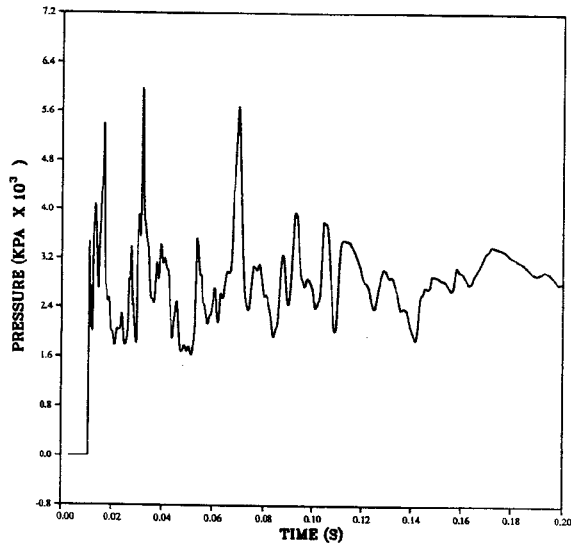

Figure 17. Experimental data overpressure record from Station 26. The same record as shown in Figure 14, but at a different scale
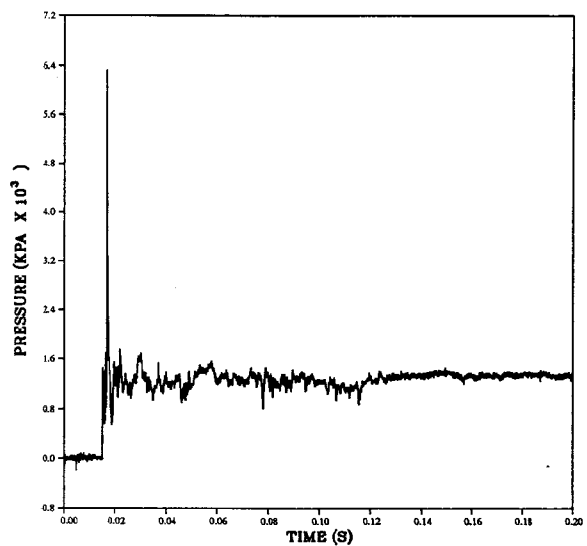

Figure 18. SHARC calculation overpressure record from Station 17, in the left adit near the entrance to Chamber #2

Figure 19. Experimental data overpressure record from Station 17, in the left adit near the entrance to Chamber #2
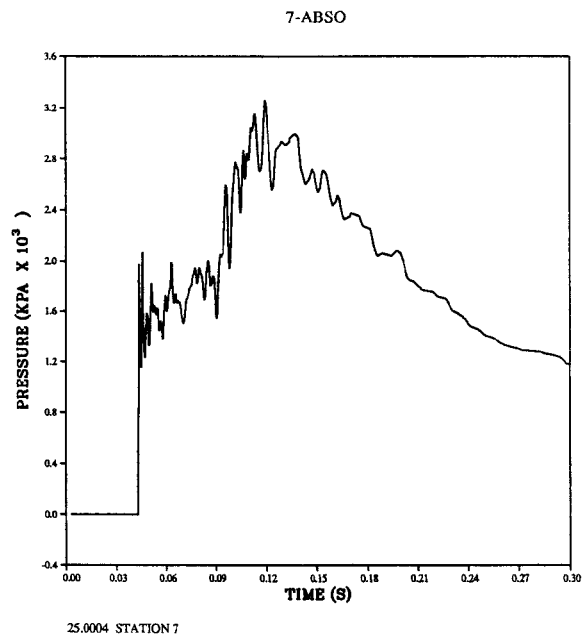
FIGURE 20. AND FIGURE 21.

7-ABSO

25.0004 STATION 7

Figure 20. SHARC calculation overpressure record from Station 7, in the main tunnel
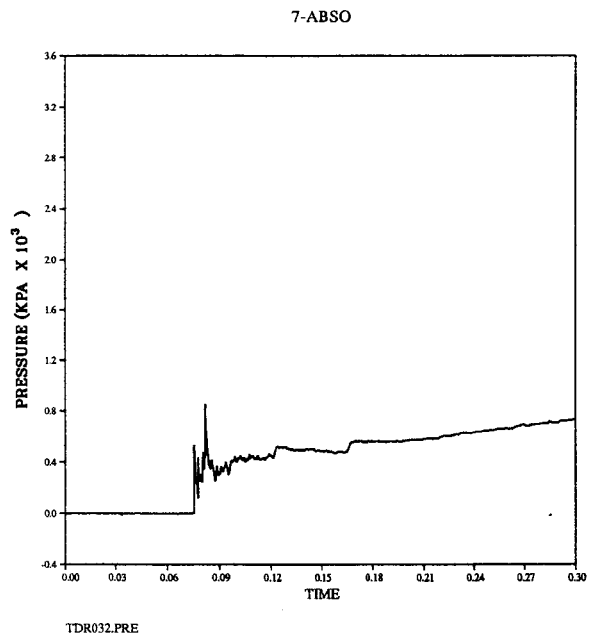
7-ABSO

TDR032.PRE

Figure 21. Experimental data overpressure record from Station 7, in the main tunnel